

PACS 63.20.dk, 75.50.Dd, 75.50.Pp

Vibrational states of hexagonal ZnO doped with Co

I.M. Kupchak, N.F. Serpak, V.V. Strelchuk, D.V. Korbutyak

*V. Lashkaryov Institute of Semiconductor Physics, National Academy of Sciences of Ukraine,
45, prospect Nauky, 03680 Kyiv, Ukraine, e-mail: kupchak@isp.kiev.ua*

Abstract. Vibrational density of states of 12.5% cobalt doped bulk hexagonal ZnO has been studied using the density functional theory method. It has been shown that introduction of cobalt into ZnO leads to appearance of additional vibrational modes with their frequencies dependent on the relative positions of cobalt atoms. The magnetic and vibrational properties have been studied in highly Co-doped ZnO samples that are characterized by a high possibility of metal clusters formation.

Keywords: ferromagnetism, ZnO, vibrational mode, diluted magnetic semiconductors.

Manuscript received 04.09.14; revised version received 02.12.14; accepted for publication 19.02.15; published online 26.02.15.

1. Introduction

Zinc oxide (ZnO), due to the wide direct band gap ($E_g \sim 3.3$ eV) at RT, large exciton binding energy ($E_x \sim 60$ meV) and strong excitonic emission, is widely used as a material for filters and detectors of UV radiation [1, 2]. It also remains a promising material for photovoltaic systems. ZnO quantum dots (QD) show stable quantum yield of luminescence even at room temperature. Due to ability to bind chemically with organic molecules, QDs can serve as effective optical labels for biomedical applications, especially in combination with plasmon enhancement of Raman scattering [3].

Doping with transition metal atoms opens another field of ZnO QDs applications. Diluted magnetic semiconductor QDs are interesting materials for spintronics. They can serve as memory cells and even as the logic elements for data processing due to their ability to store both electric charge and spin. The range of possible magnetic impurities is rather wide. It includes Fe, Co, Mn, Ni, Cr, and V impurities, but the most interesting is the Co case. Historically, Co doped ZnO is

the first semiconductor with theoretically predicted and experimentally confirmed magnetic properties at room temperature [4, 5]. Despite ZnO is already well-studied and widely used in technology, the nature of its magnetic properties, which appear due to transition metals doping, is still far from clear understanding. In particular, although ZnO:Co demonstrates mainly ferromagnetic properties at the room temperature, paramagnetic and antiferromagnetic properties also have been observed [6, 7]. The situation becomes even more complicated in the case of low-dimensional systems. Due to appearance of additional surface states, the magnetic and electronic properties of such systems will be determined also by the surface-to-volume ratio.

It is clear that magnetic properties of ZnO:Co should depend on the relative position of neighboring cobalt atoms [8]: if two atoms are close to each other, then their spins are likely antiparallel resulting in the antiferromagnetism of the system; if cobalt atoms are rather isolated from each other, the ferromagnetic state of the system is mainly realized.

One of the most informative methods for studying such structural disorders is the Raman light scattering. In

particular, micro-Raman studies are applicable even in the case of nanocrystals [9-12], while the X-ray analysis does not always allow to identify their structure distinctly.

In contrast to undoped ZnO samples, Raman spectra of ZnO:Co samples demonstrate additional bands between LO and TO phonon modes, the intensity of which increases with the Co atom concentration. In particular, in [9] two additional bands in the ranges 470...500 and 550...600 cm^{-1} have been observed. The first band could be ascribed to the surface optical phonon modes [9, 13]. Another band is associated with resonant Raman effect under subband Co^{2+} *d-d* transitions.

In another work [10], Raman scattering spectra of ZnO:Co show two additional bands, but their position is somewhat higher: 723 and 669 cm^{-1} . Authors have found that the first line is an element sensitive vibrational mode related with Co_{Zn} substitution. The second line could be attributed to cobalt – oxygen vacancy – cobalt complexes, since its intensity is decreasing after oxygen annealing. In other studies [14, 15] Raman scattering spectra contain bands at 194, 480, 519, 617, and 689 cm^{-1} , which correspond to the bands of spinel Co_3O_4 [16]. This fact indicates the presence in the ZnO:Co films of a secondary phase in the form of CoO or Co_3O_4 clusters. In general, there are various data in the literature on the positions of the additional bands in ZnO:Co spectra, even for the samples obtained in the same way. This is due to the fact that the samples could have a polycrystalline structure, contain other impurities or native defects that can form cobalt complexes.

To verify the above assumptions and explain the nature of these additional bands, we performed calculations of vibrational states on the base of density functional theory. In our calculations, the first band at 470...500 cm^{-1} should not appear under the assumption of its surface phonon nature, since we consider the bulk material. Instead, the presence of the second band may indicate the involvement of the cobalt atoms into formation of the given vibration modes.

2. Calculations and discussion

Following [8], we examined a 32-atomic supercell (denoted as a “sample” in what follows) of hexagonal ZnO, which was generated by $2 \times 2 \times 2$ repeated translations of the primitive cell along the directions of elementary translations. The lattice parameter ($a_0 = 3.2497 \text{ \AA}$) and the volume of the unit cell correspond to those determined experimentally. To simulate doped ZnO, we replaced in the initial sample (sample “init”) two zinc atoms with cobalt atoms, thus forming the chain Zn–O–Co (sample “far” with larger distance between Co atoms), and the chain Co–O–Co (sample “near” with shorter distance between Co atoms) as shown in Fig. 1. To simulate complex “cobalt – oxygen vacancy – cobalt” defect, we have removed in a sample “near” one oxygen atom, which connects cobalt atoms (sample “vac”).

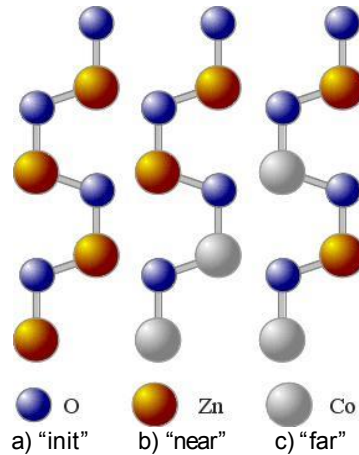


Fig. 1. Structural elements of the samples under studying (colour). For B/W : large dark yellow — Zn ions, large light grey — Co ions, small dark blue — O ions.

The number of cobalt atoms in the samples corresponds to the 12.5% cobalt concentration. It is known that cobalt atoms, being introduced with a high concentration into ZnO, form clusters, and thus the high degree of doping can be obtained. Hence, the case of a sample “near”, in which cobalt atoms are placed close to each other, reflects this possibility. Sample “far” describes the case where the cobalt atoms form single impurity substitutions Co_{Zn} , so the Coulomb interaction between them is eliminated (or reduced).

Electronic structure of ZnO:Co semiconductor was investigated by the method of density functional theory (DFT) using the generalized gradient approximation (GGA) implemented in the Quantum-Espresso software package [17]. We have used ultrasoft Perdew-Burke-Ernzerhof pseudopotentials [18] with 12 valent electrons for zinc (including 3*d* shell), 6 valent electrons for oxygen, and 9 valent electrons for cobalt. Besides, $4 \times 4 \times 3$ Γ -centered special grid of points in the *k*-space generated by the Monkhorst-Pack scheme [19] and Methfessel-Paxton smearing technique [20] with the smearing parameter of 0.005 Ry for the Brillouin zone integration used in our calculations. The kinetic energy cutoff of 40 Ry was used to expand the wave functions in terms of plane waves. Systems were relaxed through all internal coordinates until the Hellmann-Feynman forces became less than 10^{-4} a.o., keeping the form and volume of supercell fixed.

In our calculation, geometric optimization showed that Co_{Zn} substitution does not lead to significant changes in the position of atoms in the unit cell. Similar results were obtained in [8, 21], although in [8] it was noted that when doping ZnO with other 3*d*-impurities, geometric optimization is very important in the study of the magnetic properties. To verify this, we performed additional calculations of the total energy for the “near” system. Thus, after a more precise geometrical optimization of the system by using the $4 \times 4 \times 3$ *k*-point grid and 45 Ry kinetic energy cutoff, it was found that

ZnO:Co is ferromagnetic in this configuration, and the difference between antiferromagnetic (AF) and ferromagnetic (FM) states is about 4 meV. A somewhat different situation arises if such calculations are done using the Hubbard model. In this case, the lowest energy state of the considered configuration is the antiferromagnetic one, but even in this case the difference between FM and AF states is negligible. Nevertheless, we performed the calculations of vibrational states of the systems in AF configuration without using the Hubbard model.

Fig. 2 demonstrates the calculated density of vibrational states of initial and doped with Co atoms ZnO. The spectra have been obtained using the Lorentz line broadening with the half-width of 3 cm^{-1} , since in this case the comparative analysis and classification of these lines according to the terms of symmetry is somewhat difficult, which is caused by a large number of vibrational modes. Furthermore, it is noteworthy that the resulting density of vibrational states contains all possible modes (not just those allowed in Raman or IR spectra) making the comparison with experiment a tedious task. However, one can see from the figure that introduction of cobalt atoms into bulk ZnO leads to appearance of the additional oscillating modes, resulting in the redistribution of the vibrational density of states towards the higher frequencies. In particular, the vibrational density of states of the “init” system (Fig. 2a) has the maximum at 450 cm^{-1} that is close to the frequency of the mode E_2^{high} (437 cm^{-1}) in ZnO [22]. In the case of the “far” system (Fig. 2b), this maximum appears already at 500 cm^{-1} , and in the case of the “near” system (Fig. 2c) it shifts even further to the region of 550 cm^{-1} . For the system containing the “cobalt – oxygen vacancy – cobalt” chain (Fig. 2d), no vibrational modes above 600 cm^{-1} are observed within the framework of our model, and therefore we cannot confirm the conclusions made by authors of the work [10] about the responsibility of these complexes for the band at 699 cm^{-1} . Thus, we can say that such a type of the complexes Co–O–Co, as were created in the “near” system, are responsible for the appearance of the additional broad band within the region $550 \dots 600 \text{ cm}^{-1}$, which can be observed in the experiment.

To determine the behavior of the density of vibrational states when the cobalt atoms form large clusters in ZnO, we have performed calculations of the vibrational modes frequencies in 4-atom unit cell using the same values of all other parameters like to the case of 32-atomic system. Fig. 3 demonstrates the vibrational mode frequencies of bulk ZnO (black lines). To simulate the cobalt clusters, we replaced all zinc atoms with cobalt, keeping the atomic positions and lattice structure the same as in ZnO. Geometric optimization and frequency calculations were carried out for the FM and AF states of the system separately. Of course, these calculations are somewhat naive and do not take into account many factors, including the fact that the cobalt

clusters are surrounded by ZnO. As in the previous case, the replacement of zinc atoms with the cobalt ones does not change essentially the position of atoms in the unit cell. However, now the ground state is the AF state, and the difference between the total energy of AF and FM states is $\sim 60 \text{ meV}$.

The frequencies of vibrational states in hexagonal ZnO and CoO in FM and AF states are shown in Fig. 3. The CoO system in both the AF (blue line) and FM (red line) states shows the vibrational modes with frequencies between TO and LO modes presented in Fig. 2. In the AF state, these vibrational modes are closer to the LO mode than the corresponding modes in the FM state and are well separated from the TO mode. In the case of FM state, these modes are observed in the region corresponding to the TO mode. Therefore, we can conclude that in the case of cobalt doping ZnO with high doping levels, when cluster formation becomes possible, the system (or selected regions containing cluster) will be found in the AF state, and its vibrational density of states will contain the additional modes observed in experimental spectra between TO and LO.

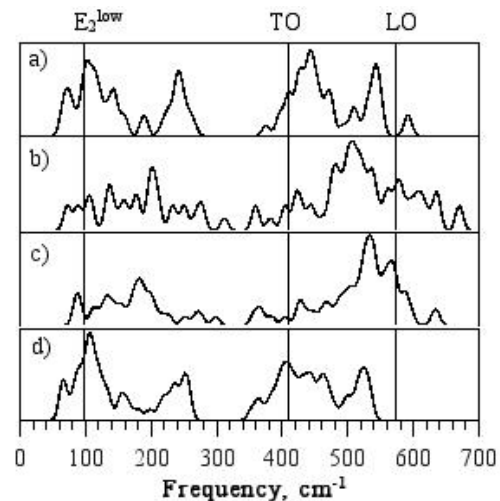


Fig. 2. Density of vibrational states of ZnO doped with cobalt: a) sample “init”, b) sample “far” c) sample “near”, d) sample “vac”.

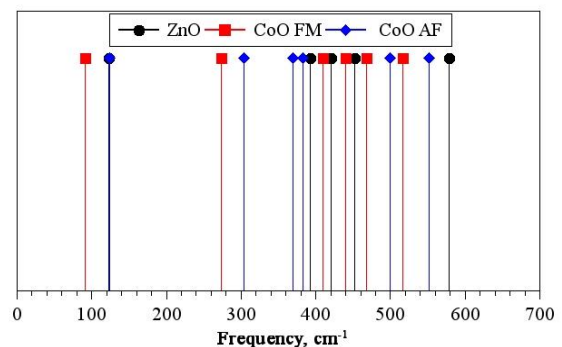


Fig. 3. Frequencies of the vibrational ferro- and antiferromagnetic states of ZnO and hexagonal CoO.

3. Conclusions

We have carried out the study of the density of vibrational states in hexagonal ZnO doped with cobalt by using the density functional theory method. We have considered various mutual positions of cobalt atoms in the structure including cases of single atoms and their complexes, as well as the possibility of cluster formation. It has been found that two cobalt atoms placed near to each other (Co–O–Co chain) lead to a redistribution of vibrational density of states, and its maximum shifts to the region of 550 cm^{-1} . Since an additional band is observed in this region of the Raman scattering spectrum of ZnO:Co, we can say that this band is formed by the vibrational states of the Co–O–Co complex. In addition, the cobalt clustering also can lead to appearance of additional modes with the frequencies lying between TO and LO modes in ZnO, which are associated with the vibrations of Co–O–Co chains.

Acknowledgements

The work was supported by Science for Peace and Security Program (the grant NATO NUKR.SFPP 984735).

References

1. H. Liu, V. Avrutin, N. Izyumskaya, Ü. Özgür, and H. Morkoç, Transparent conducting oxides for electrode applications in light emitting and absorbing devices // *Superlatt. Microstruct.* **48**(5), p. 458-484 (2010).
2. Ü. Özgür, Y.I. Alivov, C. Liu et al., A comprehensive review of ZnO materials and devices // *J. Appl. Phys.* **98**, p. 1-103 (2005).
3. A. Rumyantseva, S. Kostcheev, P.-M. Adam et al., Nonresonant surface-enhanced Raman scattering of ZnO quantum dots with Au and Ag nanoparticles // *ACS Nano*, **7**(4), p. 3420-3426 (2013).
4. T. Dietl, H. Ohno, F. Matsukura, J. Cibert, and D. Ferrand, Zener model description of ferromagnetism in zinc-blende magnetic semiconductors // *Science*, **287**(5455), p. 1019-1022 (2000).
5. K. Sato and H. Katayama-Yoshida, Stabilization of ferromagnetic states by electron doping in Fe-, Co- or Ni-doped ZnO // *Jpn. J. Appl. Phys.* **40**(4A), p. L334 (2001).
6. I. Djerdj, Z. Jaglicic, D. Arcon, and M. Niederberger, Co-doped ZnO nanoparticles: Minireview // *Nanoscale*, **2**(7), p. 1057-1104 (2010).
7. L. Li, Y. Guo, X. Y. Cui et al., Magnetism of Co-doped ZnO epitaxially grown on a ZnO substrate // *Phys. Rev. B*, **85**(17), 174430 (2012).
8. P. Gopal and N. Spaldin, Magnetic interactions in transition-metal-doped ZnO: An ab initio study // *Phys. Rev. B*, **74**(9), 094418 (2006).
9. V.V. Strelchuk, V.P. Bryksa, K.A. Avramenko, P.M. Lytvyn, M.Y. Valakh, and V.O. Pashchenko, Ferromagnetism in Co-doped ZnO films grown by molecular beam epitaxy: magnetic, electrical and microstructural studies // *Semiconductor Physics, Quantum Electronics and Optoelectronics*, **14**(1), p. 31-40 (2011).
10. Q. Cao, S. He, Y. Deng et al., Raman scattering investigations on Co-doped ZnO epitaxial films: Local vibration modes and defect associated ferromagnetism // *Curr. Appl. Phys.* **14**(5), p. 744-748 (2014).
11. C. Sudakar, P. Kharel, G. Lawes, R. Suryanarayanan, R. Naik, and V.M. Naik, Raman spectroscopic studies of oxygen defects in Co-doped ZnO films exhibiting room-temperature ferromagnetism // *J. Phys.: Condens. Matter*, **19**(2), 26212 (2007).
12. J. Kaur, R.K. Kotnala, V. Gupta, and K. Chand Verma, Anionic polymerization in Co and Fe doped ZnO: Nanorods, magnetism and photoactivity // *Curr. Appl. Phys.* **14**(5), p. 749-756 (2014).
13. V. Fonoberov, K. Alim, A. Balandin, F. Xiu, and J. Liu, Photoluminescence investigation of the carrier recombination processes in ZnO quantum dots and nanocrystals // *Phys. Rev. B*, **73**(16), p. 1-9 (2006).
14. J.S. Thakur, G.W. Auner, V.M. Naik, C. Sudakar, P. Kharel, G. Lawes, R. Suryanarayanan, and R. Naik, Raman scattering studies of magnetic Co-doped ZnO thin films // *J. Appl. Phys.* **102**(9), 093904 (2007).
15. H. Zhou, L. Chen, V. Malik et al., Raman studies of ZnO:Co thin films // *phys. status solidi*, **204**(1), p. 112-117 (2007).
16. V.G. Hadjiev, M.N. Illiev, and I.V. Vergilov, The Raman spectra of Co_3O_4 // *J. Phys. C: Solid State Phys.* **199**, p. 3-6 (1988).
17. P. Giannozzi, S. Baroni, N. Bonini et al., Quantum Espresso: A modular and open-source software project for quantum simulations of materials // *J. Phys.: Condens. Matter*, **21**(39), 395502 (2009).
18. J.P. Perdew, K. Burke, and M. Ernzerhof, Generalized gradient approximation made simple // *Phys. Rev. Lett.* **77**(18), p. 3865-3868 (1996).
19. J.D. Pack and H.J. Monkhorst, Special points for Brillouin-zone integrations // *Phys. Rev. B*, **16**(4), p. 1748-1749 (1977).
20. M. Methfessel and A.T. Paxton, High-precision sampling for Brillouin-zone integration in metals // *Phys. Rev. B*, **40**(6), p. 3616-3621 (1989).
21. S. Hu, S. Yan, M. Zhao, and L. Mei, First-principles LDA+U calculations of the Co-doped ZnO magnetic semiconductor // *Phys. Rev. B*, **73**(24), 245205 (2006).
22. C.F. Klingshirn, A. Waag, A. Hoffmann, and J. Geurts, *Zinc Oxide: From Fundamental Properties towards Novel Applications*. Berlin, Springer, 2010, p. 359.